Chinese Physics Letters

REVIEW

Integrable Deep Learning

Cite as: Yong Chen. 2026 *Chin. Phys. Lett.* **43** 060001

DOI CSTR

Recommended Articles

Enabling Intrinsic Antiferroelectricity in Two-dimensional $NbOCl_2$: Molecular Dynamics Simulations based on Deep Learning Interatomic Potential
Jiawei Mao, Yinglu Jia, Gaoyang Gou, Shi Liu, and Xiao Cheng Zeng
Chin. Phys. Lett. **43**, 010703 (2026)

HRR-PINN: A Deep Learning Method for Solving Complex Data-Driven Solutions
Huijuan Zhou, and Yong Chen
Chin. Phys. Lett. **43**, 040003 (2026)

Reinforcement Learning for Efficient Identification of Soliton System Parameters Across Expansive Domains
Cheng Hu, Zhiyang Zhang, Muwei Liu, Liuyu Xiang, Huijia Wu, Wenjun Liu, and Zhaofeng He
Chin. Phys. Lett. **41**, 120303 (2024)

Efficient Preparation of Fermionic Superfluids in an Optical Dipole Trap through Reinforcement Learning
Yueyang Min, Ziliang Li, Yi Zhong, Jia-An Xuan, Jian Lin, Lei Feng, and Xiaopeng Li
Chin. Phys. Lett. **42**, 100302 (2025)

A Data-Driven Adaptive Deep Learning Method for Nonlinear Schrödinger Type Equation
Shifang Tian, Yaxuan Yu, and Biao Li
Chin. Phys. Lett. **42**, 120001 (2025)

High-Resolution Recognition of Orbital Angular Momentum Modes in Asymmetric Bessel Beams Assisted by Deep Learning
Pengfei Xu, Xin Tong, Zishuai Zeng, Shuxi Liu, and Daomu Zhao
Chin. Phys. Lett. **41**, (2024)

A series journal of Chinese Physical Society distributed by IOP Publishing

Chinese Physics Letters

Chin. Phys. Lett. **43** 060001 (2026)

REVIEW

DOI: 10.1088/0256-307X/43/6/060001
CSTR: 32039.14.0256-307X.43.6.060001

Integrable Deep Learning

Yong Chen(陈勇)[1,2,*]

[1]College of Mathematics and Systems Science, Shandong University of Science and Technology, Qingdao 266590, China
[2]School of Mathematical Sciences Key Laboratory of Mathematics and Engineering Applications (Ministry of Education) and Shanghai Key Laboratory of PMMP, East China Normal University, Shanghai 200241, China

[*]Corresponding author. Email: ychen@sei.ecnu.edu.cn

We explain the motivation for proposing the concept and framework of integrable deep learning (IDL), and focuse on a series of advances we have made in IDL algorithms. 1. Two-stage PINN methods based on conservation laws, and PINN methods based on the Miura transformation; 2. Lax pair-informed neural networks (LPNNs) and DT-LPNN combined with the Darboux transformation; 3. Novel convolutional neural network architectures for integrable systems, including pseudo grid-based physics-informed convolutional-recurrent network (PG-PhyCRNet) and polynomial extractor for rogue wave patterns (PE-RWP).

Introduction

The development of nonlinear science is closely intertwined with the advancement of computer science. Research in nonlinear science primarily encompasses three areas: solitons, chaos, and fractals. In 1953, Fermi, Pasta, and Ulam, using the early computer MANIAC-I, discovered the recurrence phenomenon of FPU [1]. In 1963, Lorenz discovered the celebrated Lorenz chaotic phenomenon while performing numerical simulations on the LGP-30 computer [2]. In 1965, Kruskal and Zabusky performed computer simulations of the mathematical model underlying the FPU problem, giving rise to the concept of the "soliton" [3]. This achievement heralded the genuine revival of modern integrable systems theory and laid the foundation of modern soliton theory, representing a significant advance in the study of nonlinear systems. In the 1970s, Mandelbrot employed IBM computers to produce the first rendering of the celebrated Mandelbrot set [4]. The ongoing interaction between computer science and nonlinear science will continue to generate breakthroughs in fields such as artificial intelligence and quantum simulation. History demonstrates that many transformative scientific discoveries have emerged from the confluence of "computational experimentation" and theoretical insight-a paradigm that constitutes the core methodology of modern scientific research. The four paradigms of science are a concept introduced by Turing Award laureate Jim Gray to describe the evolution of scientific research methodologies. This framework posits that scientific paradigms are continuously transformed by technological progress, with each new paradigm not supplanting its predecessor but rather extending the frontiers of scientific exploration: the First Paradigm, Empirical Science; the Second Paradigm, Theoretical Science; the Third Paradigm, Computational Science; and the Fourth Paradigm, Data-Intensive Science. Future scientific inquiry may advance toward a "Fifth Paradigm", exemplified by AI-driven autonomous research.

In 2024, Hopfield and Hinton were awarded the Nobel Prize in Physics for their development of foundational methods underpinning modern machine learning through the application of physical theory. In 1982, Hopfield drew upon physics describing the properties of matter to devise a neural network-the Hopfield network [5]. His work was particularly informed by the study of magnetic materials, whose physics is grounded in atomic spins, whereby each atom behaves as a microscopic magnet. The description of the entire network is equivalent to the energy of spin systems in physics, and the network is trained by identifying connection values between nodes such that stored patterns correspond to states of low energy. Hinton, widely regarded as a founding figure of artificial intelligence, built upon the Hopfield network and incorporated the Boltzmann distribution from statistical physics to propose the "Boltzmann machine" [6]. Their work demonstrates that physics is not only a tool for exploring natural laws but also a conceptual paradigm driving the technological revolution. This recognition foreshadows the trajectory of future scientific development-interdisciplinary integration will serve as the central engine of breakthrough discovery. Physical methodologies are employed to address problems in artificial intelligence, while AI technology in turn becomes an instrument of physical research. This bidirectional interaction blurs disciplinary boundaries and has engendered the newly emerging paradigm of "AI for Science".

In recent years, scientific machine learning has emerged as a new discipline. Physics-informed machine learning (PIML) [7] has emerged as a novel paradigm that deeply integrates physical knowledge with data-driven approaches in response to this development. By embedding prior knowledge-such as physical laws, conservation principles, and system structures-directly into machine learning models, PIML enables models to learn simultaneously from observational data and physical laws, thereby achieving an organic unification of data-driven and mechanism-driven approaches. Compared with conventional methods, PIML reduces data requirements while enhancing model interpretability, computational efficiency, and generalization robustness, opening a new technical pathway for addressing complex problems in scientific computing and engineering applications. Research in PIML can be organized into three principal directions. The first involves utilizing neural networks as novel tools for the numerical solution of partial differential equations (PDEs), achieving efficient simulation through the learning of solution functions, operator mapping, or reduced-order modeling [8,9]. The second concerns the inversion of mathematical and physical laws or system parameters from observational data, enabling the identification and modeling of unknown dynamical systems [10,11]. The third focuses on innovative neural network architecture design that explicitly preserves the intrinsic geometric structures and symmetries of physical systems [12]. These three directions collectively constitute the theoretical and methodological framework of PIML. From the discovery of new particles in high-energy physics experiments to weather forecasting, astronomical research, and the simulation of complex systems, machine learning permeates virtually every domain of physics.

The research group of Karniadakis at Brown University systematically proposed the Physics-Informed Neural Network (PINN)

Received 6 April 2026; accepted 25 April 2026; published 10 June 2026
© 2026 Chinese Physical Society and IOP Publishing Ltd. All rights, including for text and data mining, AI training, and similar technologies, are reserved.

Check for updates

framework in 2019 [8]. The PINN algorithm employs automatic differentiation to embed physical prior information-expressed through governing equations-directly into the loss function required for network training, thereby enforcing a specific output structure. By leveraging the strengths of deep learning, PINN achieves high-accuracy solutions to both forward and inverse PDE problems using limited training data together with governing equations. In the forward problem, an approximate solution to the PDE is obtained; in the inverse problem, unknown parameters within the PDE model are identified.

In 2019, Chen proposed the concept and framework of integrable deep learning (IDL) and led his PhD student team to conduct a series of related studies. The principal motivations were threefold. First, integrable systems possess a rich sample space consisting of classical exact solutions-particularly localized wave solutions such as solitons, breathers, and rogue waves. Second, they exhibit elegant structures, endowed with infinitely many symmetries, infinitely many conservation laws, Lax pairs, Painlevé truncations, and nonlinear superposition formulas for solutions. Third, they are supported by classical theories and solution methodologies, including inverse scattering transforms, Darboux transformations, bilinear methods, and symmetry-based approaches. Since then, our group has conducted a series of studies on IDL, which can be delineated into three progressively deepening stages. The first stage centers on the direct exploration of localized wave solutions and forward and inverse problems in integrable systems using deep learning methods such as PINN. The second stage involves organically incorporating the intrinsic structures and properties of integrable systems into the deep learning framework, achieving a qualitative transition from "tool borrowing" to "structural integration". The third stage aims at establishing a comprehensive theoretical and methodological framework for IDL, elevating artificial intelligence methods to active instruments for the discovery of novel physical laws and unknown integrability properties.

In the first stage of our research, we progressively extended our study from $(1+1)$-dimensional integrable equations to more complex scenarios involving multiple components, high dimensions, nonlocal systems, and variable coefficients. Correspondingly, our algorithmic framework evolved from standard PINN to include adaptive activation functions, domain decomposition, adaptive weights, adaptive sampling, and operator learning.

In the development of localized wave solutions and governing equations, early work focused on integrable systems in $(1+1)$-dimension, encompassing classic models such as the Korteweg-de Vries (KdV) equation, the modified KdV (mKdV) equation, the Burgers equation, the Sharma–Tasso–Olver equation, and the Sine–Gordon (SG) equation, achieving data-driven learning of soliton solutions and their interactions [13−15]. For the nonlinear Schrödinger equation (NLS), we discovered a data-driven rogue wave for the first time through deep learning methods. This work was recognized as "The Most Influential Paper of the Year" by Chinese Physics B due to its innovation and impact [16]. For the derivative NLS equation and the Chen–Lee–Liu equation, we further learned more complex nonlinear localized waves, such as breathers, rogue waves, and periodic rogue waves [17−19]. As system complexity increased, our investigations extended to multi-component coupled systems, including vector rogue waves and bright-dark solitons of the Manakov system [20], and interactions among vector waves in the Yajima–Oikawa system [21], as well as to higher-dimensional integrable models, such as lump solitons of the $(2+1)$-dimensional Kadomtsev–Petviashvili(KP) equation and resonant rogue waves of the reduced KP equation [22]. For nonlocal integrable systems with $\mathcal{PT}$-symmetry, we incorporated $\mathcal{PT}$-symmetric constraints into the loss function to effectively overcome the challenge that nonlocal derivative computations pose to network training, leading to the development of the PTS-PINN framework, specifically designed to handle nonlocal equations [23]. This framework was successfully applied to solve both forward and inverse problems for the nonlocal Hirota equation, nonlocal mKdV equation, nonlocal NLS equation, nonlocal three-wave interaction equation, and nonlocal Sasa-Satsuma equation [24−26]. For the forward problem in the variable coefficient setting, we successfully recovered abundant wave structures including variable coefficient solitons and variable coefficient kinks. For the corresponding inverse problems, we advanced from inferring constant parameters to discovering functional coefficients, and successfully identified multiple forms of variable coefficients: polynomial, trigonometric, fractional, and oscillatory decaying, from variable coefficient versions of the KdV equation, SG equation, KP equation, NLS equation, Burgers equation and Hirota equations, while also addressing cases involving multiple coexisting variable coefficients [27−30]. Furthermore, our research extended into the domains of complex fluid dynamics and quantum physics, where we learned various internal wave structures (internal solitary waves, internal breathers, and internal rogue waves) governed by the $(2+1)$-dimensional three-coupled Davey–Stewartson system and the KP equation [31,32], as well as modulation of single quantum droplets, interference patterns of multiple quantum droplets, and breather excitations on a droplet background described by the Gross–Pitaevskii equation [33].

In the development of algorithmic techniques, to address the vanishing gradient and slow convergence induced by strongly nonlinear terms, we introduced neuron-local adaptive activation functions and proposed an improved PINN algorithm to enhance the expressive capacity of the network [17]. To overcome the multi-scale problems arising from internal waves, we introduced adaptive weights based on Gaussian probability, resolving the loss imbalance issue during training and enabling the simultaneous learning of internal waves and velocity potentials [31,32]. To handle the complexity introduced by variable coefficients, we added hard constraints on variable coefficients through a dual-network architecture and employed a ResNet structure to unify linear and nonlinear coefficients. We further introduced strategies such as gradient enhancement and transfer learning to strengthen the network's ability to capture gradient features and improve the accuracy of variable-coefficient identification [28−30]. To mitigate error accumulation and instability in large spatiotemporal scale evolution, we proposed a time-piecewise PINN based on pseudo-initial-value points, significantly improving model performance over long temporal domains to handle the complex dynamics of quantum droplets [33]; we improved the bc-PINN algorithm, modifying the loss function to ensure backward compatibility and thereby more accurately capturing the transient, steep dynamical features of high-order rogue waves [34]; we also proposed a causality-respecting adaptive sampling method based on a temporal weighting function that explicitly encodes causal principles, enabling the model to progressively extend to later time points only after being sufficiently trained at earlier ones, greatly enhancing its performance on time evolution problems [35]. To discover Lax pairs from noisy data, we constructed a library of operator candidates and, through sparse optimization combining alternating direction optimization and sequential thresholding regression, learn the corresponding evolution operators [36]. To accelerate the computation of reflection coefficients in numerical inverse scattering, we designed corresponding neural operators, termed JostONet, for the high-, intermediate-, and low-energy regimes based on DeepONet and MIONet, and incorporated physical priors such as normalization conditions, conservation properties, and hard boundary constraints, providing a promising alternative for the computation of reflection coefficients [37].

Additionally, in the field of integrable systems, other Chinese scholars have conducted a series of important studies using PINN. A two-stage initial-value iterative neural network has been proposed to compute solitary wave solutions of nonlinear wave equations using only initial values [38]. A residual-based adaptive PINN has been developed, which adaptively samples high-error regions via residuals to achieve high-accuracy solutions for soliton and rogue wave dynamics [39]. A physics-based meta-learning method has been proposed to enhance neural network initialization for soliton parameter identification, substantially reducing errors in both fundamental and dissipative soliton systems [40]. A T-CRNN hybrid network framework has been developed to enable end-to-end prediction from laser cavity physical

parameters to optical soliton evolution [41]. Transformer-enhanced PINN have been proposed to accurately solve both forward and inverse problems of the Fokas–Lenells equation with improved convergence [42]. A pre-fixed multi-stage training scheme has been developed by integrating error measurement, multi-stage optimization, and adaptive weighting strategies, demonstrating superior approximation capability and accelerated convergence [43]. The informed reconstruction-oriented numerical network has been proposed by incorporating both a finite-difference-based numerical loss term and a clustering reconstruction mechanism [44]. The distortion of the Peregrine soliton under a Gaussian-type perturbation in the initial condition has also been investigated using PINN [45]. A convolutional neural network has been used to predict the number of solitons from short-time evolution data of the NLS equation [46]. Based on a multi-stage augmented Lagrangian PINN, the prediction of coaxial bubble coalescence in multiphase flow has been achieved [47]. The SPINN incorporates invariant surface conditions from Lie or non-classical symmetries into the PINN framework, significantly improving accuracy for both forward and inverse PDE problems [48]. Adaptive residual point distribution in weighted PINN leads to the A-WPINN algorithm, improving accuracy by an order of magnitude for coupled nonlinear wave equations [49]. In the XPINN domain decomposition method, the interface line is replaced by a small interface zone to better capture the dynamical behavior of localized waves [50]. An adaptive sampling physics-informed neural network has been proposed for the simulation of high-order rogue waves [51]. The second stage of IDL aims to embed integrable structures and properties into neural networks. The following sections of this paper will focus on three key aspects of this stage.

Physics-Informed Neural Network Algorithms Based on Conservation Laws and Miura Transformations

The loss function of the standard PINN method imposes only local constraints at a finite set of collocation points, making it difficult to capture the deep physical structure of the governing equations in a global sense. The remarkable properties intrinsic to integrable systems offer a promising avenue for addressing this limitation. Integrable systems possess a wealth of distinctive features, such as infinitely many conserved quantities and classical transformations, all of which encode strong prior constraints on the solution space. Failing to exploit these structures forces the neural network to operate purely as a general-purpose approximator, blindly fitting data without guidance, thereby squandering the intrinsic physical priors embedded in the integrable structure and compromising the physical reliability of the resulting numerical solutions. To this end, we conduct systematic research along two directions within the framework of IDL: (1) we leverage the conserved quantities of integrable systems to propose a two-stage PINN methodology that enforces global constraints, thereby improving both the accuracy and generalization capability; (2) we embed Miura transformations into the neural network architecture to achieve unsupervised, data-driven solving across different equations, and further exploit the many-to-one mapping nature of such transformations to discover novel localized wave solutions (kink-bell type) of the mKdV equation.

The Two-Stage PINN Method Based on Conserved Quantities. A remarkable property of integrable systems is the possession of infinitely many conserved quantities. Obtained via spatial integration of conservation densities, conserved quantities naturally encode global information about the solution over the entire spatial domain, making them ideal vehicles for incorporating global physical constraints into the neural network loss function. To this end, we propose a two-stage PINN method based on conserved quantities [52], which embeds the conserved quantity constraints of integrable systems into the neural network training process for the first time, thereby enabling the imposition of physical constraints from a global perspective.

The core innovation of this method lies in decomposing the PINN solving process into two stages. In the first stage, a standard PINN is trained with the sum of mean squared errors for the initial-boundary data and the equation residual as the objective function:

$$\mathrm{MSE}_1 = \mathrm{MSE}_u + \mathrm{MSE}_f, \tag{1}$$

yielding a preliminary numerical solution $\hat{u}_1(x,t)$. In the second stage, conserved quantity constraints are introduced on top of this foundation. Specifically, for a given conservation density $M[u]$ of the equation, the corresponding conserved quantity $m(t) = \int \mathcal{M}[u]\,\mathrm{d}x$ must be independent of time t. A global constraint term MSE_m is constructed by measuring the deviation of the conserved quantity from its initial value $m(t_0)$ at N_c randomly sampled time instances, and is incorporated into the second-stage loss function together with the term MSE_s (which quantifies the discrepancy between the solutions of the two stages):

$$\mathrm{MSE}_2 = \mathrm{MSE}_u + \mathrm{MSE}_f + \mathrm{MSE}_s + \mathrm{MSE}_m, \tag{2}$$

where

$$\mathrm{MSE}_s = \frac{1}{N_s}\sum_{i=1}^{N_s} |\hat{u}(x_s^i, t_s^i) - \hat{u}_1(x_s^i, t_s^i)|^2, \tag{3}$$

$$\mathrm{MSE}_m = \frac{1}{N_c}\sum_{i=1}^{N_c} |m(t_m^i) - m(t_0)|^2. \tag{4}$$

The necessity of the two-stage design stems from the following consideration: if the conserved quantity term is incorporated directly into the original PINN, the optimization process will be dominated by MSE_m, causing convergence to a suboptimal local minimum and yielding results inferior to the original PINN. The two-stage strategy instead leverages the coarse solution $\hat{u}_1$ from the first stage to stabilize the optimization landscape, after which the second stage breaks out of the first-stage convergence state under the global constraints imposed by the conserved quantities, thereby searching for a superior opti-mum. The conserved quantities are computed via numerical quadrature:

$$m(t_0) = \int_{x_0}^{x_1} \mathcal{M}[u](x,t_0)\mathrm{d}x \approx \sum_{j=2}^{N_x} \mathcal{M}[u](x^j,t_0)\frac{x_1 - x_0}{N_x - 1}, \tag{5}$$

$$m(t_m^i) = \int_{x_0}^{x_1} \mathcal{M}[\widehat{u}](x,t_m^i)\mathrm{d}x \approx \sum_{j=2}^{N_x} \mathcal{M}[\widehat{u}](x^j,t_m^i)\frac{x_1 - x_0}{N_x - 1}. \tag{6}$$

The technical flowchart of this method is presented in Fig. 1.

The method has been systematically validated on multiple integrable equations, including the Boussinesq–Burgers equation and the Sawada–Kotera equation, successfully reproducing a variety of localized wave solutions such as soliton solutions, interaction solutions, soliton molecules, M-shaped double-peak solitons, plateau solitons, and single-peak solitons. Numerical experiments demonstrate that, relative to the baseline PINN, the proposed method achieves error reductions ranging from 18% to nearly 80%, with accuracy improvements of up to one order of magnitude in certain cases. The stability of the method is further corroborated through repeated experiments under different random initialization seeds. Moreover, compared to a transfer learning strategy that fine-tunes the same network, the approach of training an independent network in the second stage yields substantially superior accuracy. This advantage arises because the network parameters of the two solutions can differ significantly: the pretrained weights tend to lock the optimization within the neighborhood of the first-stage local minimum, whereas independent training affords the second stage considerably greater freedom to explore the parameter space.

This work represents the first incorporation of conserved quantities of integrable systems into neural network training, opening a new pathway for systematically embedding the deep physical structure of integrable systems into data-driven solvers, and offering important reference value for subsequent PINN improvement research targeting integrable systems.

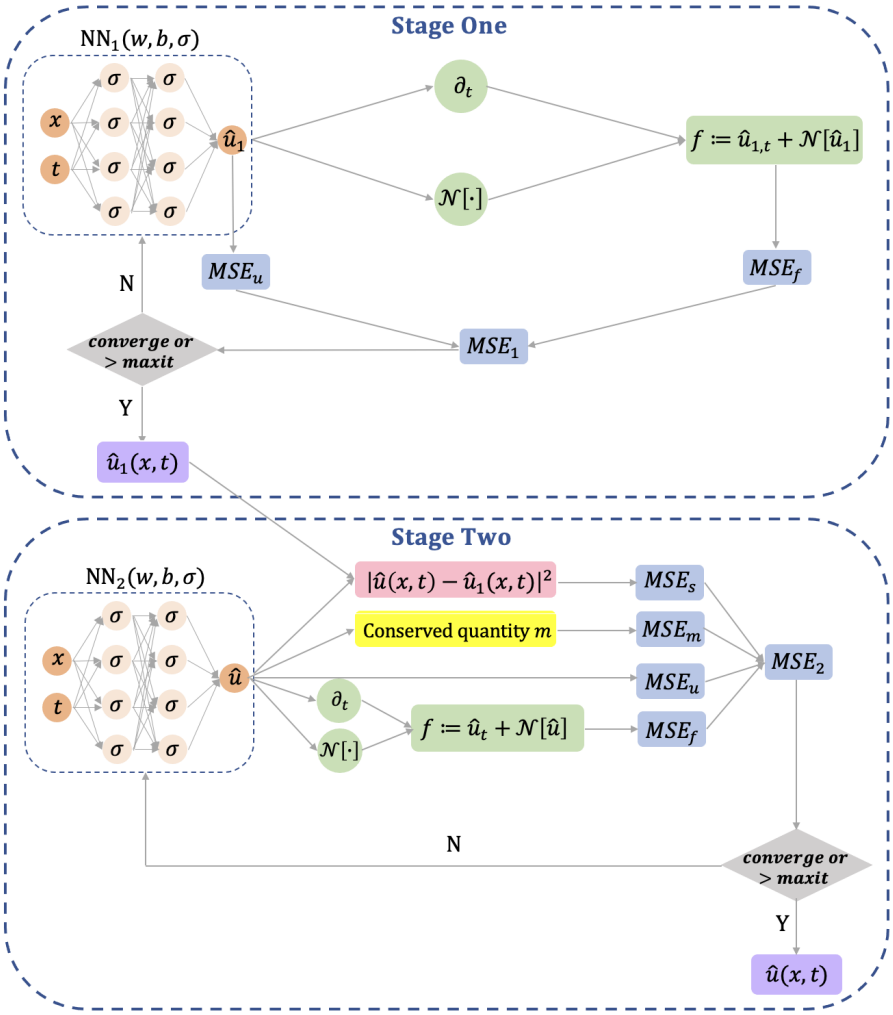

Fig. 1. Schematic diagram of the two-stage physics-informed neural network method based on conserved quantities.

The PINN Methods Based on Miura Transformations and Discovery of New Localized Wave Solutions. Another important direction in IDL concerns the incorporation of classical transformation theory from integrable systems into the PINN framework. The most significant transformation in this context is the Miura transformation, which, in the form of an explicit nonlinear mapping, establishes a bridge between the solutions of the two most prominent integrable equations-the mKdV equation and the KdV equation. The best-known example, proposed by Miura (1968), maps the solution v of the defocusing mKdV equation

$$v_t - 6v^2 v_x + v_{xxx} = 0 \tag{7}$$

to the solution u of the KdV equation

$$u_t + 6uu_x + u_{xxx} = 0 \tag{8}$$

via the explicit nonlinear transformation $u = v_x - v^2$. More generally, for a pair of nonlinear PDEs

$$F(u, u_x, u_t, \cdots) = 0, \quad G(v, v_x, v_t, \cdots) = 0, \tag{9}$$

a Miura transformation is a mapping $v \mapsto u = T(v, v_x, v_t, \cdots)$ such that any solution of the first equation yields a solution of the second, which can be written as a constraint

$$M(v, v_x, v_t, \cdots, u) = 0. \tag{10}$$

Traditionally, this transformation has been employed to generate solutions of one equation from known solutions of another. However, recovering v from the initial-boundary data of u alone involves implicit expressions that are analytically intractable. We propose two PINN-based schemes that incorporate the Miura transformation constraint directly into the neural network architecture (see Fig. 2), enabling a data-driven solution of this inverse procedure [53]. The resulting framework is cast as an unsupervised learning paradigm for v, requiring no initial or boundary information on v whatsoever.

To implement the above idea, we propose two concrete schemes. In Scheme 1, a single neural network is constructed with both u and v as outputs. The loss function comprises four terms: the initial-boundary data loss $\mathrm{MSE_u}$ for u, the KdV equation residual $\mathrm{MSE_F}$, the mKdV equation residual $\mathrm{MSE_G}$, and the Miura transformation constraint $\mathrm{MSE_M}$. Joint minimization of all four terms drives the network to simultaneously satisfy the dynamical constraints of both equations and enforce the transformation relation exactly, yielding $\hat{u}(x,t)$ and $\hat{v}(x,t)$ simultaneously.

Scheme 2 adopts a two-stage strategy. In the first stage, u is solved by a standard PINN, producing a high-accuracy numerical solution $\hat{u}(x,t)$. In the second stage, the numerical information furnished by $\hat{u}$ serves as a surrogate for the initial and boundary data of v, and a second network is trained independently with a loss function consisting solely of the mKdV equation residual $\mathrm{MSE_G}$ and the Miura transformation constraint $\mathrm{MSE_M}$. This sequential procedure decouples the two learning tasks while circumventing the need for any direct observations of v.

A systematic comparison of the two schemes reveals complementary characteristics. Scheme 1 is structurally simpler and incurs lower training cost, achieving marginally superior accuracy in relatively straightforward settings such as the real Miura transformation. However, when the constraints are more numerous and the equation

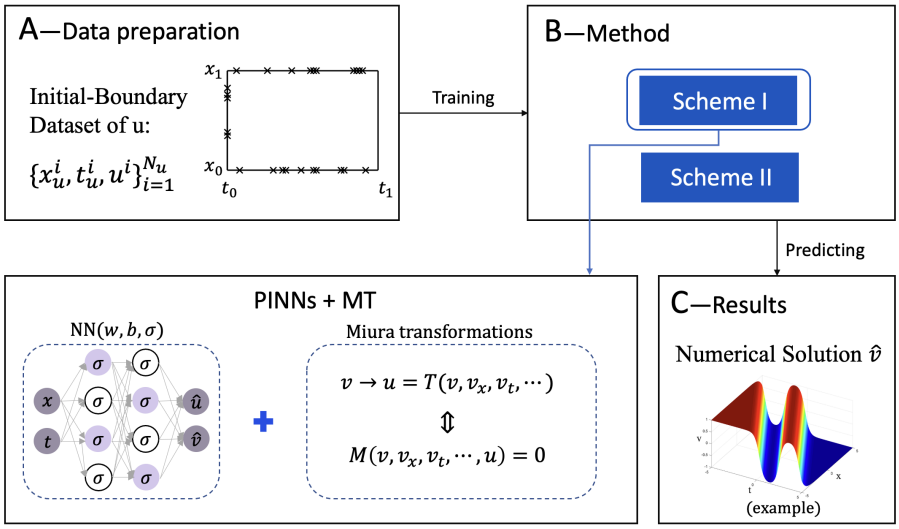

Fig. 2. Illustrations of problem-solving process.

structure more complex—as in the complex Miura transformation involving complex-valued solutions—the multi-objective optimization of a single network becomes insufficiently stable, leading to a substantial degradation in accuracy. Scheme 2 distributes the difficulty across two independent networks through task decomposition, with the architecture of the second network amenable to flexible adjustment. In the complex-valued setting, Scheme 2 achieves accuracy that is on average approximately two orders of magnitude higher than that of Scheme 1, while also exhibiting significantly greater computational efficiency, with a relative computational cost typically below 0.4.

Among the findings of this work, the most significant arise from the many-to-one mapping property of the Miura transformation. Taking the initial-boundary data of the single-soliton solution of the KdV equation as input, the implicit equation $v_x - v^2 = u$ admits multiple distinct solutions for v. Remarkably, this process yields kink-bell type solutions of the mKdV equation that, to the best of our knowledge, have not been previously observed or reported in the literature, constituting a genuinely novel class of localized solutions. The validity of these data-driven solutions is confirmed by verifying that the mean squared error of the equation residual is of order 10^{-7}, and that the three-dimensional distribution of the PDE residual over the full spatiotemporal grid remains of order 10^{-3}, both of which establish that all recovered solutions satisfy the mKdV equation. Different neural network architectures—varying in the number of hidden layers and neurons per layer—as well as different spatiotemporal domains, are shown to influence the type of solution obtained, vividly demonstrating the interplay between the diversity of neural network solutions and the many-to-one nature of the Miura transformation.

This work represents one of the first systematic attempts to integrate classical transformation theory in integrable systems with PINN, offering a new avenue for the a priori exploration of novel solutions to integrable equations via deep learning methods. The unsupervised solution framework, the treatment of implicit transformations, and the discovery of new localized wave solutions collectively carry significant implications for the methodological enrichment of IDL, while also laying the groundwork for further investigations into the combination of other classical transformations—such as the Darboux transformation and the reciprocal transformation—with the PINN methodology.

Integrable Deep Learning Methods Based on Lax Pairs and Darboux Transformations

Integrable systems possess rich mathematical structures and distinctive properties. The Lax pairs stands as one of the most fundamental features in the theory of integrable systems: it not only provides the theoretical foundation for developing a general framework of inverse scattering theory, but also propels the advancement of integrable systems theory and established its significant role in mathematical physics and related disciplines. The Darboux transformation (DT) method is one of the most fundamental and important methods for solving localized wave solutions of integrable systems. Focusing on the Lax pairs and DT method, we have carried out the following work: (1) we proposed Lax pairs informed neural networks (LPNNs), including LPNN-v1 and LPNN-v2, and investigated the forward problems of a series of important and representative integrable equations; (2) by combining LPNNs with the DT theory of integrable systems, we proposed the DT-based LPNN (DT-LPNN) and discovered new localized wave solutions.

Solving Integrable Systems via Lax Pairs Informed Neural Networks. As an equivalent linear representation of integrable systems, the Lax pairs contains richer and more structured prior information, it can to a certain extent replace the model constraints of the original integrable system itself, or also provide additional linear structural constraints. Accordingly, developing novel IDL methods by leveraging Lax pairs information in conjunction with powerful deep neural networks constitutes a highly distinctive and promising research direction.

We proposed LPNNs applicable to integrable systems with Lax pairs [54], it mainly consists of two schemes: LPNN-v1 employs only the Lax pairs equations as the source of Lax pairs information, whereas LPNN-v2 incorporates both the Lax pairs and its compatibility condition/zero-curvature equation as Lax pairs information. Each scheme carries its own distinctive advantages: LPNN-v1 directly solves the linear Lax pairs equation and achieves substantially improved computational efficiency for integrable systems with relatively simple Lax pairs, while LPNN-v2 is designed for integrable systems with more intricate Lax pairs and attains higher training accuracy. The complete network workflow of LPNNs is illustrated in Fig. 3.

The numerical experiments encompass a number of highly important and representative integrable systems together with their rich localized wave solutions, including soliton solutions of the KdV and mKdV equations, rogue wave solution of the NLS equation, kink solution of the SG equation, non-smooth peakon solution of the Camassa-Holm equation, pulse solution of the short-pulse equation, line soliton solution of the KP equation, and lump solution of higher-dimensional KdV equations. The results demonstrate that the training time of LPNN-v1 is two to five times faster than that of the standard PINN, while LPNN-v2 achieves markedly higher accuracy than both the standard PINN and LPNN-v1. These findings not only validate the effectiveness and superiority of LPNNs in solving integrable systems, but also highlight their latent capability in addressing associated spectral problems.

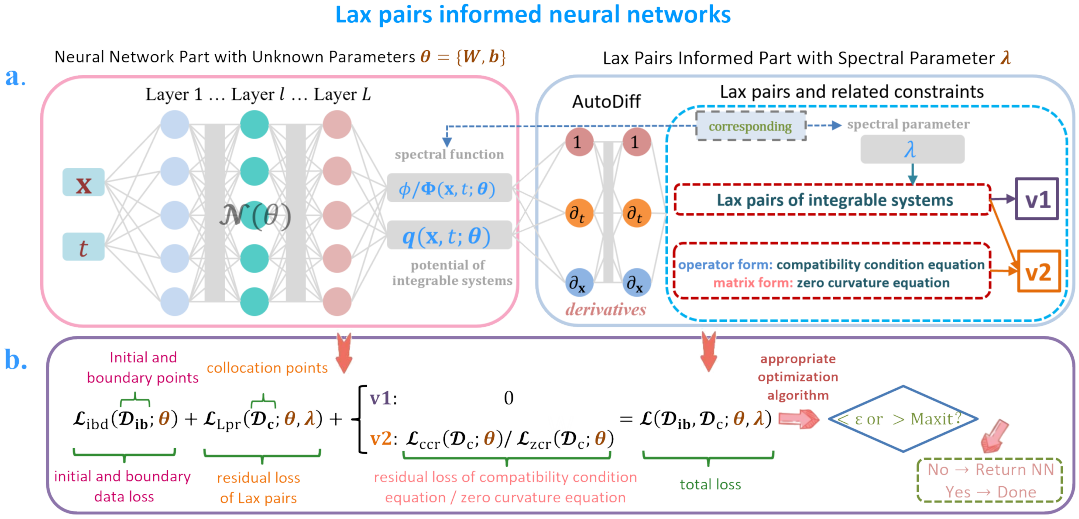

Fig. 3. PNNs method technical flowchart.

Constructing New Localized Wave Solutions via Darboux Transformation-Based LPNN. In the study of localized waves in integrable systems, the discovery of new nonlinear localized waves has long been an important problem in both the theory and applications of integrable systems. The classic DT method usually selects trivial seed solutions to precisely construct common localized wave solutions, while new nonlinear local wave solutions may often need to be constructed starting from complex seed solutions. Within the classic DT framework, it confronts significant analytical computational bottlenecks, severely limiting the discovery and exploration of novel nonlinear localized wave solutions.

Motivated by the spectral problem-solving capability of LPNNs, and making full use of the obtained spectral parameters and corresponding spectral functions, we incorporated DT theory into the LPNNs framework and proposed the DT-LPNN method [55]. The DT-LPNN method starts from a nontrivial seed solution and embeds the DT formulas associated with the seed solution, spectral parameter and the spectral functions obtained from the neural network part into the DT part of the DT-LPNN, then reconstructs new Lax pairs information part and a corresponding loss function, and force the newly generated solution to satisfy the compatibility condition/zero curvature equation of the Lax pairs to ensure its reliability, thereby generates new nonlinear localized wave solutions. The core advantage of DT-LPNN lies in its ability to broaden the solution search space of integrable systems while maintaining training accuracy, thus providing an effective approach for the discovery of novel nonlinear localized wave solutions.

In the numerical experiments, we applied the DT-LPNN method to study the Kraenkel–Manna–Merle system and its spectral problem, obtaining high-accuracy data-driven seed solutions, spectral parameter and spectral functions, from which new nonlinear localized wave solutions were generated. Taking a bright single-soliton solution as the nontrivial seed solution, we generated a new dark single-soliton solution on a variable nonzero background wave. Furthermore, using a two-soliton solution as the nontrivial seed solution, we constructed a localized wave solution exhibiting dynamics distinctly different from those of the original two-soliton solution.

The two IDL methods described above demonstrate the application of Lax pairs in the design of deep neural networks: LPNNs achieve efficient and high-accuracy solutions of integrable systems and their spectral problems by incorporating Lax pairs information; DT-LPNN further builds upon the spectral problem-solving capability of LPNNs by integrating DT theory, enabling the discovery of new nonlinear localized wave solutions from nontrivial seed solutions. The two works are hierarchically progressive and mutually reinforcing, fully embodying the innovative paradigm of embedding the intrinsic properties and theoretical methods of integrable systems into the architectural design of deep neural networks. They provide both theoretical and methodological references for the further development of IDL methods, and open viable pathways toward the discovery of new localized wave solutions and the solution of spectral problems in integrable systems.

Novel Convolutional Neural Network Architectures for Integrable Systems

With the rapid advancement of machine learning in the field of PDEs, the research paradigm is shifting from classical analytical derivation towards data-driven feature extraction and evolutionary simulation. Convolutional neural networks (CNNs), owing to their outstanding feature extraction capability and weight-sharing mechanism, have demonstrated tremendous potential in handling integrable systems that exhibit spatiotemporal evolution. By incorporating the structural properties of integrable systems, we have designed novel CNN architectures and conducted research along two main directions: (1) the numerical evolution of discrete integrable systems; (2) the discovery of intrinsic mathematical structures embedded in rogue wave patterns.

PG-PhyCRNet for the Forward Problem of Discrete Integrable Systems. Traditional scientific computing typically discretizes continuous equations via finite-difference schemes, a process that often faces formidable challenges regarding stability and convergence. In contrast, discrete integrable systems possess inherent integrable discretization schemes that preserve physical attributes such as conservation laws at the discrete level. A prominent framework for handling such systems is the physics-informed convolutional recurrent network (PhyCRNet), constructed by combining CNNs with recurrent neural networks.

Discrete integrable systems reduce to their continuous counterparts when taken in the continuum limit. Taking the Toda lattice equation as an illustrative example:

$$\dot{u}_n = u_n(v_n - v_{n-1}), \quad \dot{v}_n = u_{n+1} - u_n. \tag{11}$$

Under an appropriate step-size parameter δ and a suitable change of variables, this system converges to the celebrated KdV equation in the continuum limit. Similarly, the self-dual network equation reduces to the mKdV equation in the same limit. Consequently, numerical solutions of discrete systems can reveal the dynamical behavior of solutions to continuous integrable equations. Unlike conventional finite-difference schemes, discrete integrable equations naturally possess a globally consistent integrable structure, thereby obviating the need for additional stability and convergence analysis.

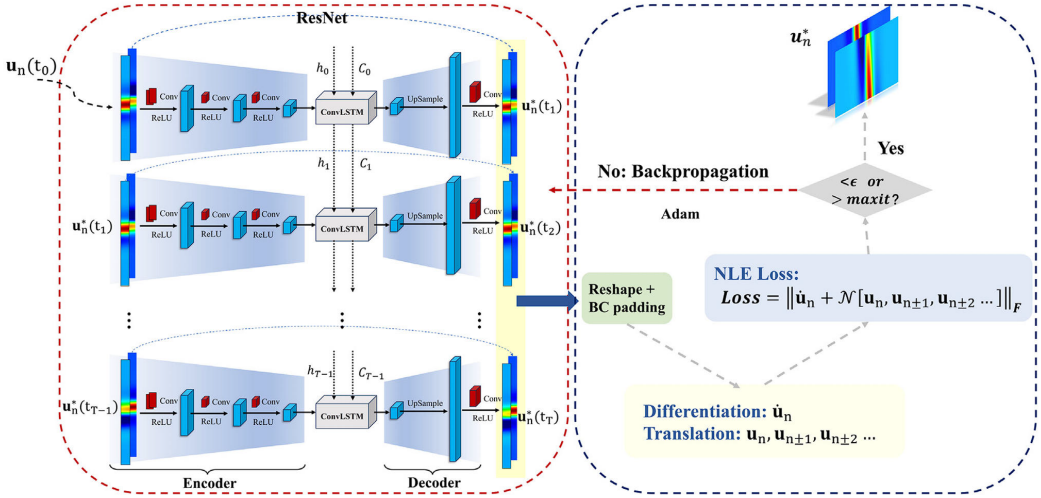

Fig. 4. Chain-like structure of ConvLSTM.

Motivated by the structural properties of discrete integrable systems, we propose the PG-PhyCRNet framework, which integrates the PhyCRNet architecture with a pseudo-grid training strategy specifically designed for solving discrete integrable lattice equations [56]. The core architecture consists of three components: an encoder (one-dimensional convolutional layers), a ConvLSTM layer, and a decoder (pixel shuffling followed by large-kernel convolution). The model updates the lattice potential function through an autoregressive process:

$$u_n(t_{i+1}) = u_n(t_i) + \delta_t \cdot \mathcal{F}[\cdot], \tag{12}$$

where $\mathcal{F}$ denotes the trained network operator. The physics-informed loss function is defined as the mean squared error (MSE) of the residual of the lattice equation:

$$\mathcal{L}_{\text{physics}} = \frac{1}{N_{\text{T}}N}\sum_{i=0}^{N_{\text{T}}-1}\sum_{j=0}^{N-1}\left|\hat{u}_{nj} + \mathcal{N}[u_{nj}, u_{nj\pm1}, \cdots]\right|^2. \tag{13}$$

The introduction of *pseudo-grid points* represents the core innovation of this method. For solitons with high wave speeds and steep profiles, the irregular distribution of integer grid points makes it difficult for the model to capture the potential function characteristics near wave crests, leading to extrapolation failure. By incorporating non-integer pseudo-grid points in the spatial domain,

$$\Omega' = \left[n_1,\ n_1 + i\frac{n_N - n_1}{N_n - 1}\right], \tag{14}$$

the network learns the global trend of the continuous potential function and replaces shift operators with appropriate slicing operations, thereby substantially enhancing its temporal extrapolation capability. The complete workflow of PG-PhyCRNet is illustrated in Fig. 4.

Numerical experiments were performed on the single-soliton and double-soliton solutions of the Toda lattice equation, as well as the rational soliton solution of the self-dual network equation. The results demonstrate that PG-PhyCRNet possesses strong extrapolation capability for multi-soliton solutions of discrete integrable equations. The interpretable physical mechanism underlying this performance is as follows: the weight sharing of CNNs enables the continuous potential-function trends learned from pseudo-grid points to constrain predictions at integer grid points; when the soliton width is narrow, the coverage of steep crest regions by pseudo-grid points allows the convolutional kernels to more effectively capture the evolutionary dynamics of the soliton.

PE-RWP for Discovering Intrinsic Mathematical Structures in Rogue Wave Patterns. Uncovering the intrinsic mathematical structures of nonlinear phenomena is one of the most important problems in AI for Science. Rogue wave phenomena in integrable systems typically exhibit highly ordered geometric patterns. Mathematical proofs have established that the geometric structure of high-order rogue wave patterns of the nonlinear NLS equation is completely determined by the zero distribution of the Yablonskii-Vorob'ev polynomial hierarchy. We propose the PE-RWP network architecture, which automatically extracts deep mathematical regularities from the solution structures of integrable systems-specifically, the discovery of mathematical structures underlying rogue wave patterns [57].

We introduce a generalized polynomial form containing two arbitrary parameters:

$$|\Delta_i| \times \left(d_i^{[k]}\right)^{-i(i+1)} = \mathcal{P}_i^{[k]}\left(z; \gamma_{i,1}^{[k]}, \gamma_{i,2}^{[k]}\right) + O\left(|a_{2k+1}|^{-1/(2k+1)}\right),\ |a_{2k+1}| \to \infty, \tag{15}$$

where $|\Delta_i|$ denotes a determinant, a_{2k+1} is a large parameter and $d_i^{[k]}$ is a real number. The key significance of this generalized design is twofold: the polynomial can describe rogue wave patterns under arbitrary rotation transformations, and it fixes the output layer of the neural network to only two learnable neurons, thereby converting a high-dimensional variable-output problem into a fixed-output multi-task learning problem.

The PE-RWP framework adopts an innovative dual-branch network architecture. The first branch (regression branch) establishes a mapping from pixelated rogue wave patterns to the polynomial parameters $\gamma_{i,1}^{[k]}, \gamma_{i,2}^{[k]}$; the second branch (classification branch) identifies the order i and arrangement type k of the rogue wave pattern. The model directly maps pixelated rogue wave pattern images to the polynomial feature space. The two branches jointly output the target generalized polynomial; the training loss function is a combination of the regression mean squared error and the multi-class cross-entropy:

$$\mathcal{L} = \frac{1}{N_{\text{b}}N_{\text{c}}}\sum_{i,k,j}\left|\hat{\gamma}_{i,j}^{[k]} - \gamma_{i,j}^{[k]}\right|^2 - \frac{1}{N_{\text{b}}}\sum_{i,\text{c}} y_{i,\text{c}}\log p_{i,\text{c}}, \tag{16}$$

where $\widehat{\gamma_{i,j}^{[k]}}$ is the predictive value and $y_{i,c}$ denotes the one-hot data.

Peregrine soliton localization, as an application of the PE-RWP framework, employs a two-stage unsupervised strategy. In the first stage, the polynomial zeros output by PE-RWP provide geometrically plausible initial positions; by asymptotic theory, the discrepancy between these zeros and the true soliton coordinates is of the order $O\left(|a_{2k+1}|^{-1/(2k+1)}\right)$, a higher-order infinitesimal. In the second stage, a feedforward neural network learns this higher-order correction, with the loss function constrained by the wave-field amplitude $|q(x_j,t_j)|$ obtained via Cardinal spline interpolation: the predicted coordinates (x_j,t_j) are required to satisfy $|q(x_j,t_j)| \geq 3-\varepsilon$ and to correspond to local maxima. The technical workflows of both neural network components are presented in Fig. 5.

In the task of discovering polynomial structure, PE-RWP success-

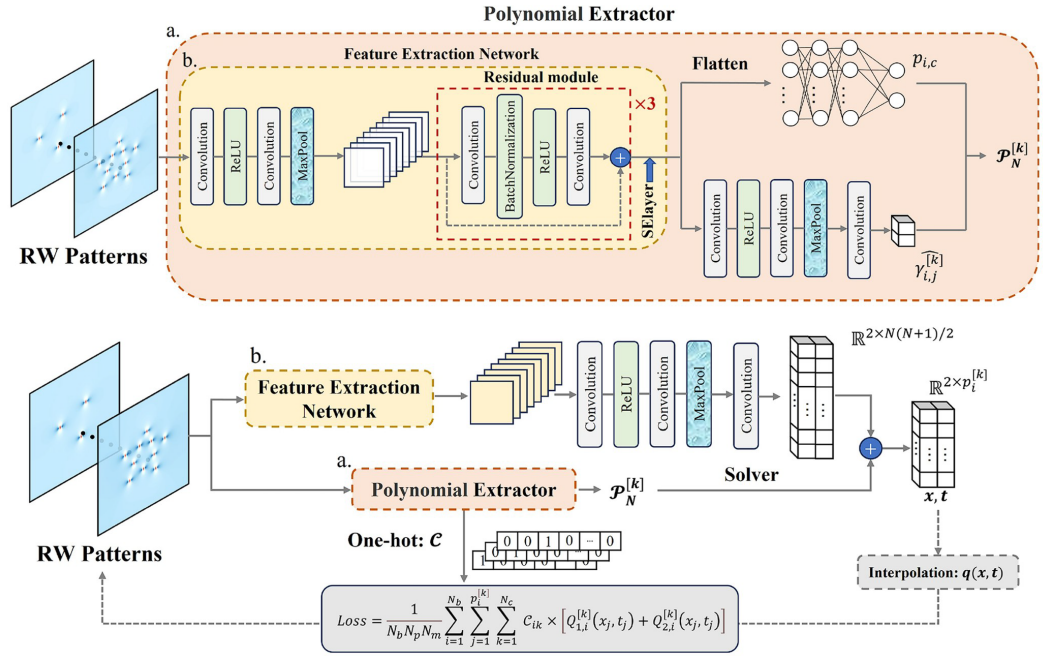

Fig. 5. Technical flowchart for PE-RWP (top) and the Peregrine wave positioning framework (bottom).

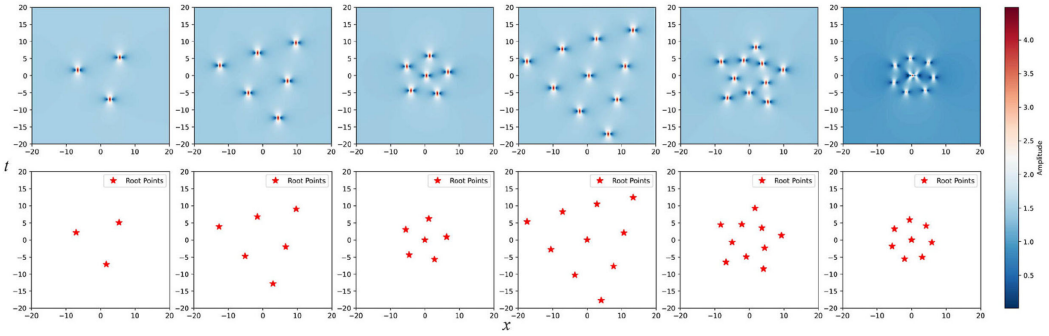

Fig. 6. Predicted polynomial results. The first row shows the input rogue wave patterns; the second row shows the zero distributions of the polynomials output by PE-RWP.

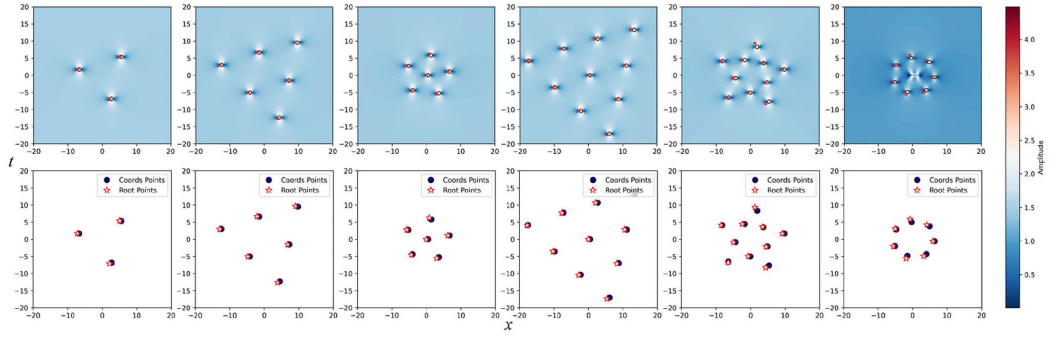

Fig. 7. Peregrine soliton localization results. The first row shows the input rogue wave patterns; the second row presents the corresponding localization results. Red asterisks indicate the distribution of polynomial roots output by PE-RWP in the complex plane; black open circles indicate the predicted positions of the Peregrine solitons.

fully establishes an automatic mapping from rogue wave patterns to their underlying polynomial structures, thereby replacing in a data-driven manner the traditionally cumbersome analytical derivations based on large-parameter asymptotic expansions. Experimental results on six geometric pattern classes from second- to fourth-order rogue waves demonstrate that the zero distribution of the generalized polynomial $\mathcal{P}_N^{[k]}\left(z;\gamma_{i,1}^{[k]},\gamma_{i,2}^{[k]}\right)$ output by the network is in excellent agreement with the spatial arrangement of the individual Peregrine solitons within the corresponding rogue wave pattern (see Fig. 6). This result reveals that the geometric regularity exhibited by the N-th order rogue wave solution of the NLS equation under large-parameter conditions is fundamentally encoded in the complex zero structure of the generalized polynomial, and that the neural network is able to directly read and output this abstract intrinsic mathematical structure from the pixel information of the pattern.

In the Peregrine soliton localization task, figure 7 presents the localization results for various rogue wave pattern arrangements of different orders randomly selected from the test set, all of which demon-

strate a high degree of accuracy. Moreover, the prediction errors of the proposed network approach the benchmark results obtained under fine grid resolution-implying that the network captures peak position information within a very short computation time that traditional methods can only reveal at the limit of computational resources.

Taken together, the two works presented above demonstrate the potential of convolutional neural networks in the study of integrable systems from complementary perspectives. PG-PhyCRNet achieves high-accuracy temporal solving and extrapolation of lattice soliton solutions through physics-informed discrete learning, while PE-RWP leverages a dual-branch architecture combined with large-parameter asymptotic theory to automatically identify the polynomial characteristics of N-order rogue wave patterns and to realize rapid unsupervised localization of Peregrine solitons. Both works embody the core idea of embedding the deep mathematical structures of integrable systems into neural network design. In particular, the PE-RWP network opens a new avenue for IDL to uncover further intrinsic mathematical structures.

Conclusion

This paper centers on the new research direction of IDL that we have pioneered, and systematically reviews the theoretical explorations and methodological practices that deeply integrate the rich intrinsic mathematical structures of integrable systems with deep learning approaches. The study shows that incorporating integrable structures-such as conservation laws, the Miura transformation, Lax pairs, the Darboux transformation, integrable discretization, and the polynomial structures of rogue-wave patterns-not only significantly improves the efficiency and accuracy of neural network solvers, but also endows data-driven methods with the ability to discover novel localized wave solutions and extract deeper mathematical structures. As the theoretical framework of IDL continues to mature, the deep integration of artificial intelligence and nonlinear science is expected to foster breakthrough discoveries across a broader range of problems in mathematical physics, providing important support for the development of the “AI for Science” paradigm.

Acknowledgements

The author sincerely thanks his doctoral student team, especially Juncai Pu, Shuning Lin, Zhe Lin, and Zhengwu Miao for their assistance, as well as Engui Fan and Qingping Liu for their valuable suggestions. This work was supported by the National Natural Science Foundation of China (Grant Nos. 12575002 and 12235007), the Science and Technology Commission of Shanghai Municipality (Grant Nos. 21JC1402500 and 22DZ2229014), and the Natural Science Foundation of Shanghai (Grant No. 23ZR1418100).

References

[1] Fermi E, Pasta J, Ulam S and Tsingou M 1955 *Studies of Nonlinear Problems* (Los Alamos, NM: Los Alamos Scientific Laboratory) Report No. LA-1940
[2] Lorenz E N 1963 *J. Atmos. Sci.* **20** 130
[3] Zabusky N J and Kruskal M D 1965 *Phys. Rev. Lett.* **15** 240
[4] Mandelbrot B B 1977 *Fractals: Form, Chance and Dimension* (W.H. Freeman and Company)
[5] Hopfield J J 1982 *Proc. Natl. Acad. Sci.* **79** 2554
[6] Ackley D H, Hinton G E, and Sejnowski T J 1985 *Cogn. Sci.* **9** 147
[7] Karniadakis G E, Kevrekidis I G, Lu L, Perdikaris P, Wang S, and Yang L 2021 *Nat. Rev. Phys.* **3** 422
[8] Raissi M, Perdikaris P, and Karniadakis G E 2019 *J. Comput. Phys.* **378** 686
[9] Lu L, Jin P, Pang G, Zhang Z, and Karniadakis G E 2021 *Nat. Mach. Intell.* **3** 218
[10] Lusch B, Kutz J N, and Brunton S L 2018 *Nat. Commun.* **9** 4950
[11] Liu Z M and Tegmark M 2022 *Phys. Rev. Lett.* **128** 180201
[12] Greydanus S, Dzamba M, and Yosinski J 2019 *Adv. Neural Inf. Process. Syst.* **32**
[13] Li J and Chen Y 2020 *Commun. Theor. Phys.* **72** 105005
[14] Li J and Chen Y 2020 *Commun. Theor. Phys.* **72** 115003
[15] Li J and Chen Y 2021 *Commun. Theor. Phys.* **73** 015001
[16] Pu J C, Li J, and Chen Y 2021 *Chin. Phys. B* **30** 060202
[17] Pu J C, Li J, and Chen Y 2021 *Nonlinear Dyn.* **105** 1723
[18] Pu J C, Peng W Q, and Chen Y 2021 *Wave Motion* **107** 102823
[19] Peng W Q, Pu J Q, and Chen Y 2022 *Commun. Nonlinear Sci. Numer. Simul.* **105** 106067
[20] Pu J C and Chen Y 2022 *Chaos Solitons Fractals* **160** 112182
[21] Pu J C and Chen Y 2023 *Commun. Nonlinear Sci. Numer. Simul.* **118** 107051
[22] Miao Z W and Chen Y 2022 *Mod. Phys. Lett. B* **36** 2150531
[23] Peng W Q and Chen Y 2024 *Chaos* **34** 043124
[24] Peng W Q and Chen Y 2022 *Physica D* **435** 133274
[25] Zhu J Y and Chen Y 2023 *Nonlinear Dyn.* **111** 8397
[26] Zhang W X and Chen Y 2025 *Nonlinear Dyn.* **113** 10211
[27] Zhou H J, Pu J C, and Chen Y 2023 *Nonlinear Dyn.* **111** 14667
[28] Miao Z W and Chen Y 2023 *Physica D* **456** 133945
[29] Lin S N and Chen Y 2024 *Physica D* **459** 134023
[30] Zhou H J and Chen Y 2025 *Physica D* **481** 134764
[31] Sun J C, Tang X Y, and Chen Y 2024 *Physica D* **459** 134021
[32] Sun J C, Chen Y, and Tang X Y 2024 *J. Syst. Sci. Complex.* **37** 545
[33] Pu J C and Chen Y 2023 *Physica D* **454** 133851
[34] Lin S N and Chen Y 2024 *Chaos* **34** 033139
[35] Lin S N and Chen Y 2025 *Physica D* **481** 134878
[36] Lin S N and Chen Y 2025 *Chaos* **35** 113120
[37] Miao Z W and Chen Y 2026 *Physica D* **486** 135073
[38] Song J, Zhong M, Karniadakis G E, and Yan Z Y 2024 *J. Comput. Phys.* **505** 112917
[39] Tian S F, Yu Y X, and Li B 2025 *Chin. Phys. Lett.* **42** 120001
[40] Zhang Z Y, Liu M W, Xing X W, Zhang S Z, Yan Z Y, and Liu W J 2025 *Comput. Methods Appl. Mech. Eng.* **438** 117852
[41] Jia Y H, Wang D L, Shen B, Ju Z T, Huang Q Y, Wang X P, Zhang J H, Wang Y Y, Liu W, and Dai C Q 2026 *Laser Phoyon. Rev.* **20** e03212
[42] Wang L Q and Tian S F 2026 *Chaos Solitons Fractals* **204** 117787
[43] Mo Y F, Ling L M, and Zeng D L 2022 *Phys. Lett. A* **421** 127739
[44] Wang P F, Sun Y Z, Triki H, and Zhou Q 2026 *Chin. Phys. Lett.* **43** 040004
[45] Wang J L and He J S 2022 *Phys. Lett. A* **452** 128432
[46] Wang Z and Cui S K 2022 *Phys. Lett. A* **456** 128536
[47] Sun K D, Lu G, Wang L, Yuan D W, Chen D G, and Zhao Y C 2025 *Phys. Rev. E* **112** 065306
[48] Zhang Z Y, Zhang H, Zhang L S, and Guo L L 2023 *J. Comput. Phys.* **492** 112415
[49] Qin S M, Li M, Xu T, and Dong S Q 2023 *Physica D* **443** 133562
[50] Chen J C, Song J, Zhou Z J, and Yan Z Y 2023 *Chaos Solitons Fractals* **176** 114090
[51] An H L, Xing K J, and Chen Y 2024 *Chaos* **34** 043153
[52] Lin S N and Chen Y 2022 *J. Comput. Phys.* **457** 111053
[53] Lin S N and Chen Y 2023 *Physica D* **445** 133629
[54] Pu J C and Chen Y 2024 *J. Comput. Phys.* **510** 113090
[55] Pu J C and Chen Y 2024 *Physica D* **467** 134262
[56] Lin Z N and Chen Y 2024 *Physica D* **468** 134304
[57] Lin Z and Chen Y 2025 *J. Comput. Phys.* **539** 114243